Anomalous glass transitions and stretched exponential relaxation in fused salts and polar organic compounds

J. C. Phillips
AT&T Bell Laboratories, Murray Hill, New Jersey 07974
(Received 14 April 1995)

As a glass-forming liquid is cooled below its melting point, its relaxation width normally increases and becomes more asymmetric. However, in fused salts the dielectric relaxation widths increase but become paradoxically more symmetric. A crossover from dominance of bulk relaxation to double-layer relaxation explains this anomaly. Microscopic theory also explains quantitatively the temperature and frequency dependence of the asymmetry relaxation parameter β, as well as its variation with material.

PACS number(s): 64.70.Dv, 77.84.Nh

I. INTRODUCTION

Among all glass formers, including inorganic network glasses, polymers, and anisotropic organic molecular liquids, the behavior of fused salts is the most anomalous. Normally, as a glass-forming material is supercooled below its equilibrium or effective melting point $T=T_m$, its relaxation spectrum exhibits two characteristic properties. First, the average relaxation time $\bar{\tau}(T)$ increases and eventually diverges as $T\rightarrow T_g^+$, where T_g is an appropriate glass transition temperature. Second, coupling between relaxation modes increases with decreasing T, as the accessible volume of configuration space decreases. The width of the distribution of relaxation times correspondingly increases. Empirically it has been found that this increase can be described quite accurately by one or two parameters (to be described further below) β such that $0<\beta\leq 1$, with $\beta=1$ corresponding to the relaxation of weakly coupled modes in the normal liquid in equilibrium with $T>T_m$. The increasing relaxation time width is described by decreasing values of $\beta(T)$, with β reaching a characteristic value at $T=T_g$. Often $\beta(T)$ reaches a plateau even before $T=T_g$. Behavior of this type has been observed not only experimentally in materials like Se (a prototypical polymer with no sidegroups) [1,2], but also in molecular dynamics simulations of spin glasses [3] and metallic glasses [4].

The relaxation behavior of the most thoroughly studied fused salt, KCN or $(KNO_3)_x[Ca(NO_3)_2]_{1-x}$, departs drastically from this natural scenario. The thermal glass transition, determined by scanning calorimetry [5] with a scanning rate of 10 K/min, occurs at $T=T_g=232$ K. However, a different glass transition temperature, $T=\tilde{T}_g=373$ K, has been inferred for ns relaxation times by neutron spin-echo measurements [6]. It is understandable that structural arrest may appear to occur at higher temperatures when measured at much shorter times with the neutron probe, so this result by itself is not anomalous. The anomalous behavior occurs in $\beta(T)$, which normally decreases with decreasing T. However, classic dielectric relation experiments [7] on KCN showed $\beta(T)$ increasing with decreasing T, which seems to mean a narrowing of the width of the distribution of relaxation times at the glass transition, which is very difficult to understand. Moreover, this anomalous behavior occurs only in dielectric relaxation measurements for T near the glass transition temperature T_g where $\tau(T)\gtrsim 10^{-6}$ s. Experiments carried out by other methods or at higher temperatures where $\tau(T)\lesssim 10^{-7}$ s exhibit a normal $\beta(T)$.

The main aim of this paper is to propose an explanation for this anomalous aspect of dielectric relaxation in fused salts. The classic dielectric relaxation experiments [7] already showed two anomalies, one of which is extrinsic and one of which is intrinsic. The extrinsic one, which was seen in some samples but not in others, was explained as the result of thermal contraction of the glass on quenching, which caused it to crack or to pull away slightly from the electrode surfaces. This would leave small gaps which act as a large capacitance in series with the sample. We are not concerned here with this extrinsic effect, but rather with the intrinsic effects of double layers at the electrode-electrolyte interfaces. We will show that such effects can be used to reconcile the classic dielectric low-frequency relaxation data with a great deal of more recent data taken by a wide variety of other methods. In addition, we have recently discussed [8] a microscopic model which organizes and explains systematic chemical trends in $\beta(T_g)$, and some have argued that the theory is incomplete because it does not explain the fused salt dielectric relaxation data. These data are generally regarded as anomalous compared to or are excluded from discussions [9–11] of higher-frequency data obtained by ultrasonic, light scattering, and neutron scattering experiments. However it is certainly more satisfactory to explain them in a microscopic context [11].

Most of the emphasis in the literature has been placed on the reconciliation of different values of $\tau(T)$ as measured in different experiments and fitted to a master curve [9–11]. Here we discuss primarily $\beta(T)$ and $\beta(\omega_0(T))$, where $\omega_0(T)=\tau^{-1}(T)$. We will see that whereas $\omega_0(T)$ exhibits interesting qualitative trends, $\beta(T)$ and $\beta(\omega_0(T))$ exhibit still more interesting quantitative trends which are related to the microscopic molecular structure and intermolecular forces. These trends in the case of anoma-

lous fused salt dielectric relaxation are especially informative.

II. GENERAL CHARACTERISTICS OF STRONGLY CORRELATED RELAXATION

The relaxation of a strongly correlated supercooled liquid or glass can be described in the time domain by a Kohlrausch stretched exponential

$$\phi(t)=\phi_0\exp[-(t/t_0)^{\beta}] , \quad (1)$$

or in the frequency domain by

$$\Phi(\omega)=\Phi_0(1+i\omega/\omega_0)^{\beta'} , \quad (2)$$

where Φ is a complex impedance. When the two functions ϕ and $\mathrm{Re}\Phi$ are compared, they are found to be quite similar near their peaks, and the connection between β and β' is known numerically [12].

The general behavior of $\beta(T)$ depends on the nature of the coupling of the heat bath to the relaxation observable. The simplest mathematical models of $\beta(T)$ are the spin-glass lattice models [3,13–15]. Numerical simulations and scaling theory show that in these mathematical models $\beta(T)$ has the simple form

$$\beta(T)\approx T/T_m, 0\le T\le T_m$$
$$=1, T>T_m , \quad (3)$$

with of course a small rounding for $T\sim T_m$, which we neglect. The scaling theory does not include the glass transition (structural arrest), but the numerical simulations show a clear-cut transition. Thus on some time scale, $\beta(T)=\beta(T_g)$ for $T\lesssim T_g$. This behavior is shown in Fig. 1(a). It should be mentioned that this behavior is in general not observed in experimental spin glasses, where power-law behavior (possibly associated with domains, which are omitted from the mathematical models and are not scalable) is prevalent.

More realistic models of molecular relaxation have been studied by molecular dynamics simulations [4,17–18]. In these studies the relaxation of a structure factor $S(Q,t)$ is studied for $Q\approx Q_1$, the first peak in $S(Q)$, corresponding to the nearest neighbor spacing if size misfit is responsible for the glass transition [4], to the interchain spacing if polymer chain entanglement is responsible [16], or to an average coordination number [17] if the latter is the key factor. (This would be the case for the fused salt $KCN=(KNO_3)_x[Ca(NO_3)_2]_{1-x}$.) Again $\beta(T)$ decreases from 1 at high T to $\beta(T_g)<1$ at the glass transition $T=T_g$.

Experimentally in materials such as supercooled Se, which consists primarily of chains with about 300 atoms for T near T_g, the situation is somewhat different [1]. Usually $\beta(T)$ reaches a plateau at $T=T_g'$ before the thermal glass transition temperature T_g is reached. This is because the latter is measured with scanning calorimetry on a time scale of order 10^2 s, whereas the former may be measured on a time scale of order ns, for instance, by spin-polarized neutron scattering [1]. This

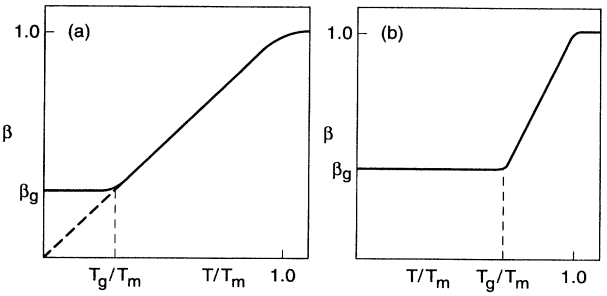

FIG. 1. (a) The norm form of $\beta(T)$ for a lattice glass such as a spin glass. To a good approximation $\beta(T)$ extrapolates to $\beta(0)=0$. (b) The normal form of $\beta(T)$ in an off-lattice glass such as an inorganic network glass, a polymer, or a fused salt. The range of $\beta(T)$ is narrowed, T_g/T_m is increased, and the plateau region below T_g may vary depending on the probe used to study the glass transition, in other words, both β_g and T_g may be probe dependent. The nature of this dependence for the fused salt KCN is discussed near the end of Sec. IV.

difference is easy to understand, as structural arrest takes place at higher temperatures on shorter time scales, but we illustrate it in Fig. 1(b) to show its relation to the lattice glass models.

Some comment is also needed concerning the meaning of T_m. Glass formation is promoted, in metallic glasses for example, by the existence of low-temperature metastable phases [18]. Then T_m may refer to the melting of microphases coupled to partial phase separation of the mixture. Thus T_m may be much lower than the melting points of KCl or $Ca(NO_3)_2$ in KCN melts, and the difference between T_g' and T_m is likely to be relatively much smaller in molecular glasses than in spin glasses, as Fig. 1 illustrates. Thus we replace Eq. (3) by the more realistic linear relation

$$\beta_\alpha(T)=\beta_{\alpha g}+(1-\beta_{\alpha g})(T-T'_{\alpha g})/(T_{\alpha m}-T'_{\alpha g}) . \quad (4)$$

III. DIELECTRIC DOUBLE LAYERS

Electrochemists have known for some time [19] that the impedance Z of a plane parallel electrolytic cell used to measure dielectric relaxation of supercooled liquids contains two parts

$$Z=Z_B+Z_D, \quad (5)$$

where the subscripts refer to the bulk melt and the electrode double layer, respectively. The impedance Z_D is sensitive to the electrode material and the double layer thickness λ is one or at most a few interfacial (or surfactant) molecular diameters [20]. If a typical cell dimension is R, the fractional volume filled by the double layer is only of order $\lambda/R\lesssim 10^{-7}$, but because of continuity of the displacement vector $\mathbf{D}$, the voltage drop across the plane parallel double layer is comparable to that across the bulk electrolyte itself. A spectacular example of dou-

ble layer impedance is that recently measured for an organic liquid mixture electrolyte and a Tl cuprate high-T_c superconductive electrode [21]. The temperature-dependent double-layer capacitance $C_D(T)$ drops rapidly (over $\Delta T < 1$ K) just above $T = T_c = 110$ K.

To describe relaxation of the plane parallel cell impedance Z we can use $\beta_\alpha(T)$ from Eq. (4) with $\alpha = B$ or D. Because the double layer is thin, we expect [22] that $T'_{Dg} \lesssim T'_{Bg}/2$ and similarly $T_{Dm} \lesssim T_{Bm}/2$. The subtle point is the relative strength of the couplings of the applied field $\mathbf{F}_a$ to the double layer and bulk relaxation modes. Let the distributions of relaxation frequencies $\omega_{0\alpha}$ be represented by $P_\alpha(\omega_0)$ and the observed distribution be $M(\omega_0)$. We represent these couplings formally by $A_\alpha(\omega_0)$:

$$A\int M(\omega_0)d\omega_0 = \int A_B(\omega_0)P_B(\omega_0)d\omega_0 + \int A_D(\omega_0)P_D(\omega_0)d\omega_0 \ . \quad (6)$$

The coupling factors $A_B(\omega_0)$ and $A_D(\omega_0)$ are not proportional to each other. This is because in the double layer there is an internal voltage differential comparable to the applied voltage, which arises from the difference in work functions between the electrode and the electrolyte. These large double-layer fields $\mathbf{F}_D$ mean that the double-layer molecular dipoles are strongly oriented normal to the double layer. So long as $\mathbf{F}_a$ is parallel to $\mathbf{F}_D$, little relaxation will occur in the double layer. However, as ω_0 decreases the wave length λ of the relaxation wave (which contains both charge and density fluctuations) will increase. From a velocity of sound $c_s \sim 10^5$ cm/sec, it follows that λ will exceed the sample dimensions R when $\omega_0 < \Omega_0 \sim 10^4\ \mathrm{s}^{-1}$. For such long wavelengths the field $\mathbf{F}_r$ associated with the relaxation wave will be partly transverse to the local surface normal. Then it will tilt the surfacant dipoles and couple $\mathbf{F}_a$ to them very strongly just because the lateral surfacant dipolar correlation length R is much larger than the melt correlation length ξ_m, with $\xi_m \lesssim 100$ Å. Indeed the relaxation wave will contain components transverse to the local surface normal at higher and lower frequencies as well, depending on the roughness of the electrode surface on depth scales of order 5–100 Å

In general we expect that $A_D(\omega)/A_B(\omega)$ will increase rapidly with decreasing $\omega_0(T)$ that is, with decreasing $T - T_g$. Thus the relaxation as $T \to T_{g+}$ will be increasingly dominated by double-layer relaxation modes, while those of the bulk melt will dominate at higher temperatures and higher relaxation frequencies ω_0.

IV. APPLICATION TO KCN

We have gathered these ideas together with the classic dielectric data ($T \gtrsim T_g$) as well as higher-temperature longitudinal dielectric modulus data from ultrasonic, Brillouin, and stimulated Brillouin scattering data in Fig. 2, which shows $\beta_\alpha(T)$ for $\alpha = B$ and D, and the crossover in the observed $\beta(T)$ which takes place between $T_g = 333$ K (calorimetric, A in the Figure) and $T = 380$ K (B in the Figure). Both $\beta_B(T)$ and $\beta_D(T)$ are normal [Eq. (4)], but

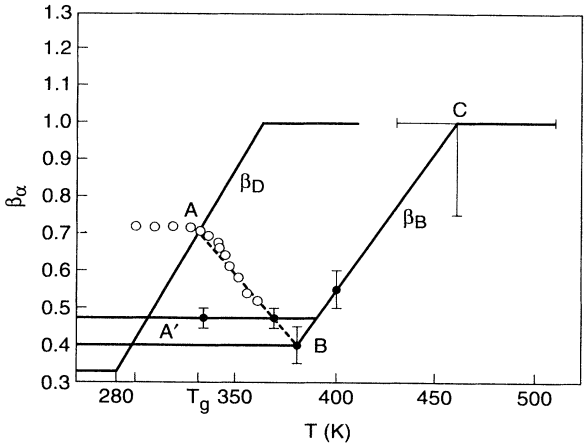

FIG. 2. The form of $\beta_\alpha(T)$ as measured by dielectric impedance spectroscopy (open circles near A), ultrasonic and Brillouin scattering data (filled circles near B and A'), and stimulated Brillouin scattering (C). Two curves for β_α are shown, for the bulk KCN melt ($\alpha = B$), and for the double layer ($\alpha = D$).

because of the crossover in coupling strengths $\beta_{AB}(T)$ is anomalous.

The construction in Fig. 2 is only schematic, because there are no independent data on $\beta_D(T)$, but there is also no reason to suppose that $\beta_D(T)$ should be qualitatively different from $\beta_B(T)$. However, there are further surprising aspects to the dielectric relaxation data which can be brought out by considering $\beta(\omega_0)$. Just as $\beta(T)$ was derived from a stretched exponential fit to measured impedances, so we can make similar fits to the derived quantities themselves, that is, carry the analysis of hindered relaxation to a higher level of abstraction. In analogy with dielectric relaxation itself we therefore relate $\beta(T)$ to $\omega_0(T)$ directly:

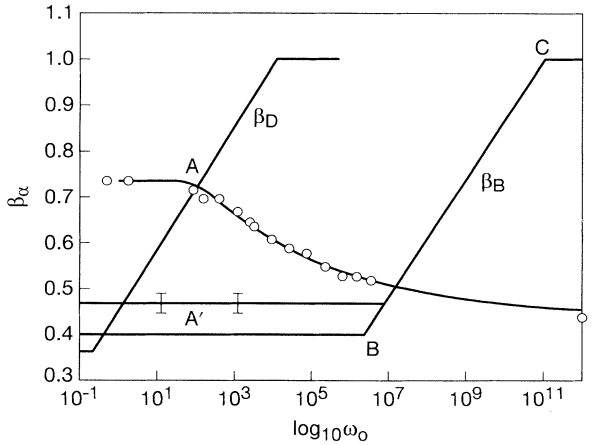

FIG. 3. The dielectric relaxation data are fitted by the solid curve using Eq. (7) of the text. The curves for β_D and β_B from Fig. 2 are also shown for convenience.

$$\beta(\omega_0)=\beta_\infty+\mathrm{Re}(\beta_0-\beta_\infty)/(1+i\omega_0/\Omega_0)^\gamma\ , \tag{7}$$

where $\beta_\infty=\lim\beta(\omega_0)$ as $\omega_0\to\infty$, and $\beta_0=\beta(0)$. For the high frequency limit at $\omega_0=10^{12}\ \mathrm{s}^{-1}$ we use the value $\beta_K=3/7$ associated with intrinsic Coulomb relaxation [8]. The results of this fit are shown in Fig. 3. The agreement is remarkable, but even more remarkable is the fitted value of the crossover frequency $\Omega_0\sim 100\ \mathrm{s}^{-1}$. This is exactly $\omega_0(T_g)$. This means that Eq. (7) in effect predicts $\beta(T)$ given $\beta(T_g)$ and $\omega_0(T_g)$ with only one adjustable parameter, which has the fitted value $\omega=0.06$. This value is much smaller than the values of $\beta\sim 0.5$ found in fitting experimental observables, but it easy to understand. It corresponds to a very wide distribution of double-layer relaxation frequencies which arises because of electrode roughness or patchiness on a scale of mm or less.

Points A, B, and C in Fig. 2 have special significance. The onset of hindered diffusive relaxation near C (430 K $<T<$ 510 K) is determined by light-scattering experiments [23] which show $\beta\approx 1$, that is, almost no asymmetry of the resonance absorption peak. At B as measured by ultrasonic absorption [24] β has dropped to 0.4, while more recent light-scattering experiment [25] for $T_g<T<T_g+40$ K have given $\beta=0.47(3)$. Taken together these two values neatly bracket the intrinsic value $\beta_K=0.43=3/7$ predicted by microscopic theory [8] for Coulomb-interaction-dominated relaxation. Also, B corresponds to the onset temperature for sharpening of the first peak at $Q=Q_1$ in the bulk structure factor $S(Q)$ as measured by spin-polarized neutron scattering [6]. At this temperature $\tau_0(T_B)\sim 10$ ns, which is the time cutoff for these experiments, so it is possible that the observed enhancement of $S(Q_1)$ for $T<T_B$ is simply due to this factor alone. However, the fact that bulk structural arrest, as measured by $\beta(T)$, reaches a plateau at $T=T_B$ suggests that this could be associated with growth of metastable microphases [18] as well. While it is difficult to separate the two effects, it is clear that for $T<T_B$ the crossover behavior in $\beta(T)$, as measured by dielectric relaxation, can be entirely associated with double layers.

To bring out the double-layer nature of the low-frequency, low-temperature dielectric relaxation described by $\beta_{AB}(T)$, in Fig. 4 we show dielectric relaxation data for a polar organic eutectic electrolyte mixture with a superconductive electrode [21]. Points A, B, and C are analogous to the respective A, B, and C points in Fig. 2. The major difference is that in Fig. 4 the low-frequency double-layer arc AB is clearly separated from the bulk arc BC, whereas in Fig. 2 the two regimes overlap somewhat. (The more complete separation in Fig. 4 may reflect a difference in electrolyte composition in the double layer and the bulk, which tends to decouple their relaxation modes.)

A characteristic feature of the present model is that it predicts that dielectric relaxation times will be shorter than thermal or viscosity-based relaxation times at the same temperatures, especially at low temperatures in the AB crossover regime where $d\beta/dT<0$. This is because thermally there is no preferential coupling of an applied

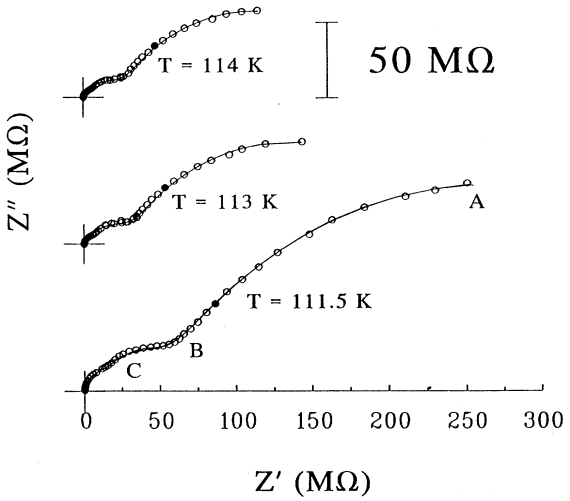

FIG. 4. Dielectric relaxation data for an organic electrolyte with a cuprate superconductor with $T_c=113$ K as reported in Ref. [21] and reproduced here for the reader's convenience. There are three arcs of size increasing from left to right as the frequency decreases. The large one on the right is assigned to the double layer, and its magnitude changes by as much as 20–30% as T passes through a ΔT range of less than 1 K at T_c, which is unambiguous evidence of a large double-layer impedance comparable to that of the bulk electrolyte. Points A, B, and C here are analogous to those in Figs. 2 and 3.

field to the double layer, so that the contribution of the double layer will be smaller than that of the bulk melt by the factor $\lambda/R\sim 10^{-7}$. The two relaxation times are compared in Fig. 5, where it can be seen that at T_g+13 K $=73\,^\circ$C the dielectric relaxation time is smaller by a factor of 10^4. Given the difference in filling factors, this means a difference in coupling strengths A_D/A_B order 10^{11} at this temperature. It is then entirely understandable why β_{AB} is anomalous when measured by dielectric relaxation.

The main concern of this paper is the anomalous behavior of $\beta_{AB}(T)$ in KCN dielectric relaxation. For completeness the issue of probe dependence of β should also be discussed for KCN. The value of $\beta(T_g)$ obtained in Brillouin scattering experiments (B in Fig. 2) is 0.4, in good agreement with $\beta_K=3/7$ for Coulomb interactions. This is what we should expect, as the Brillouin electric field $\mathbf{F}_A$ couples to charge fluctuations. A different value for $\beta_n(T)=0.58$ has been obtained in neutron spin-echo experiments [26]. These experiments span the temperature range 111–196 °C with β most sensitive to the 149–172 °C data. In the present model $\beta_n(T)$ is constant for $T\lesssim 200\,^\circ$C, in other words, the low-temperature plateau in Fig. 1(b) extends to $T\lesssim 200\,^\circ$C for the neutron data but only to $T\lesssim 110\,^\circ$C for the ultrasonic data. In the present model these differences are explained by the observation that the neutron impulse couples primarily to short-range density, not charge, fluctuations, and so one would expect the neutron experiment to give $\beta(T_g)=\beta_{\mathrm{SR}}=3/5$, which is in good agreement with observation.

The separation of charge and density fluctuations in KCN implied by theory here seems to be almost too good. However, the vibrational structure of nitrates is very different from that of halides. Balkanski, Teng, and Nusimovici [27] showed that there are three well-separated components in the optic-mode vibrational spectra of crystalline KNO_3. These are the covalent modes ($700\ cm^{-1} \lesssim \nu_c \lesssim 1400\ cm^{-1}$), the ionic modes ($\nu_i \sim 140\ cm^{-1}$), and the rotational modes ($\nu_r \lesssim 100\ cm^{-1}$). The covalent modes involve distortions of the NO_3^- complex, which ideally is an N-centered planar O equilateral triangle, while the ionic modes involve K^+—NO_3^- countermotion. Both covalent and ionic modes are admixed into diffusive acoustic modes at short wavelengths. Thus both can contribute to structural arrest near the glass transition [28]. The applied electric field $\mathbf{F}_A$ couples strongly to the low-frequency ionic modes, while neutrons are strongly scattered by the low-mass, high-energy covalent modes. Note that the equivalent temperatures for the ionic and covalent modes are respectively ~ 200 and 1000 K, respectively. Thus the observations that for KCN $\beta(T)$ when measured electrically varies rapidly for $T \gtrsim 400$ K but is essentially constant for $T \lesssim 500$ K when studied by neutron scattering are not inconsistent.

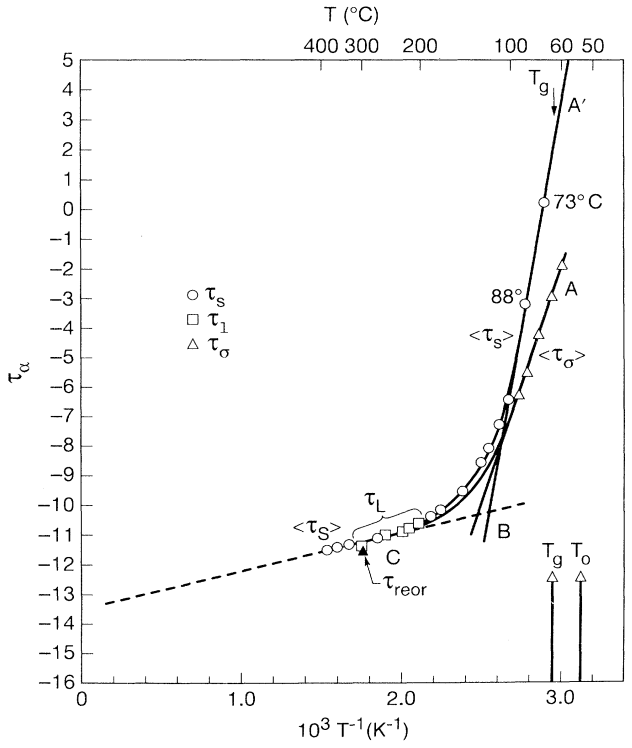

FIG. 5. This figure has been modified from Angell and Torell, Ref. [9]. It is a master curve for $\tau_\alpha(T^{-1})$, where α refers to s (viscosity), l (ultrasonic and Brillouin scattering), and σ (dielectric relaxation) data. Points A, B, and C are analogous to Figs. 2 and 3, as are the lines AB and BC. The line $A'B$ corresponds to the plateau of $\beta_B(T)$. The figure illustrates how $A'B$ is shifted to AB in the dielectric relaxation.

There is substantial phenomenological support for this model. The fused salt KCN has been thoroughly studied just because it is an exceptionally good glass former. The anion coordination numbers N_a of crystalline KNO_3 and $Ca(NO_3)_2$ are six and four, respectively. The lower coordination number enhances the glass-forming tendency ($ZnCl_2$ is a fair glass former, cation coordination number $N_c = 4$; $ZnBr_2$ is not, $N_c = 6$). Thus one would not expect that a mixture of KNO_3 into $Ca(NO_3)_2$ would enhance the glass-forming tendency were it not for the planar symmetry of NO_3, which may also promote metastable noncrystalline coordination configurations [28]. [One of the natural components for such metastable configurations is an $N_a = 5$ complex with $(Ca_2)_{1/2}$ on one side of the NO_3 plane and $(K_3)_{1/3}$ on the opposite side. This has quasipentagonal axial symmetry, and larger clusters composed of such units might develop quasi-decagonal or even partial icosahedral symmetry as alternatives to the cubic-close-packed anion symmetries of crystalline KNO_3 and $Ca(NO_3)_2$.] At the same time, the covalent NO_3 modes with $\nu_c \sim (5-10)\nu_i$ when coupled to density fluctuations, should be stable to higher temperatures than ionic modes when similarly coupled.

Molecular dynamics simulations [29] for KCN which treat the NO_3^- units as rigid have shown Kohlrausch relaxation of microscopic types which are not experimentally measurable in terms of structure factor relaxation. Both the incoherent Ca_2^+ neutron scattering factor $F_{sCa}(k_0, t; T)$ and the NO_3^- flip relaxation of π around a twofold NO_3^- axis relaxed with $\beta \approx 0.6$ for $T \sim 350$ K $\sim T_g$ for times $t \lesssim 0.2$ ns. These simulations suggest another reason for the observation of $\beta \sim 0.6$ by neutron scattering. It appears that the cation diffusive motion for T near T_g is coupled to NO_3 flips. Note that these flips do not alter the local electrical moments of the NO_3^- ions and so do not couple to the external electric fields used, for example, in ultrasonic and light-scattering experiments. In any event the conclusion that $\beta \sim 0.6$ is characteristic of short-range forces remains unchanged.

V. POLAR ORGANIC COMPOUNDS

The AB double layer to bulk crossover in dielectric relaxation, illustrated in Fig. 2 for KCN, is a general mechanism which should apply equally well to both fused salts and polar organics. In fact, $\beta(T)$ has been measured for several polar organics by dielectric relaxation [29,30] and by other methods, such as specific heat, and the low-frequency dielectric relaxation values are consistently larger than those measured in the absence of an applied field [31,32]. This suggests that double layers make a significant contribution to $\beta_\sigma(T)$ for T near T_g. The double-layer contributions are, however, smaller in the polar organics than in KCN in the sense that $d\beta_\sigma(T)/dT$ remains positive in the former. It seems likely that steric hindrance reduces the contribution of double-layer tilt relaxation modes in polar organics compared to KCN.

Relaxation data are presented by different workers in different ways. In the classic experiments [7] on dielectric relaxation in KCN, the resonance curves of $\varepsilon_2(\omega)$

were numerically fitted with the Fourier transform of the Kohlrausch stretched exponential, with β chosen to fit $\varepsilon_2(\omega)$ at frequencies near and below the peak frequency ω_p. It was noted that this procedure underestimates $\varepsilon_2(\omega)$ for $\omega \gg \omega_p$. This seems to us to be the correct procedure because it conforms best to the idea of Kohlrausch relaxation as a residual process which occurs after transients have died out. At high frequencies other relaxation processes come into play which have been discussed in terms of mode coupling [10]. We do not argue here that the mode-coupling approach is a general one which should be applied to other kinds of materials measured by other methods (where in general the Kohlrausch fit at high frequencies is much better anyway), but only that this is a useful approach to dielectric relaxation of KCN in particular, where the excess absorption at higher frequencies could easily be associated with the covalent vibrational modes of metastable clusters mentioned earlier.

Another approach that has been adopted for much recent data is a scaling one based on half-widths [33] whose main purpose seems to be to dramatize the limitations of the Kohlrausch fit at large ω/ω_p, which were already well known from the classic dielectric work [7]. In fact, the fit at higher frequencies with the Kohlrausch function seems to be better for the polar organics than for KCN. It would be interesting to know what the results for $\beta_\sigma(T)$ would have been for the polar organics had the traditional procedure been followed consistently. From the published data [33] on salol for the normalized width parameter w_σ and the approximate relation $1-\beta_\sigma = 1.047\ (1-w_\sigma^{-1})$, one can see that with decreasing T it appears that β_σ decreases most rapidly near 270 K and much more slowly between 240 and 220 K, without reaching the plateau usually found near the glass transition. There is also some evidence of an anomaly in the relaxation time in the dielectric data in the sense that Vogel-Fulcher divergence temperature T_0 shows crossover behavior starting near $\omega = 10^4\ \mathrm{s}^{-1}$, which could be related to the divergence between τ_σ and τ_α for KCN shown in Fig. 5. Again a more traditional presentation of the data would have facilitated comparison with the much better-studied case of KCN. In any event it was recognized that $\beta(T)$ as measured by specific heat and ultrasonics were in good agreement, and that the larger values found by dielectric relaxation were anomalous. Moreover, in the $\beta(T_g)$ plateau region other methods which do not couple to the double layer (specific heat, ultrasonics, two-photon correlation spectroscopy) have given $\beta = 0.60\ (8)$ for glycerol, for example [32]. This value is the one expected by theory [8], $\beta = \beta_{SR} = 3/5$, when relaxation is dominated by short-range intermolecular packing interactions.

We notice that although the fused salt KCN data are dominated by the intrinsic value $\beta = \beta_K = 3/7 = 0.43$, the polar organic intrinsic bulk behavior is usually dominated by $\beta = \beta_{SR} = 3/5$, even though the frequency dependences of the dielectric relaxation data for the fused salts and polar organics are very similar. This is not so surprising, because Coulomb interactions in the fused salts are clearly much stronger than in the polar organics, except when a strong applied field $\mathbf{F}_a$ is present in the latter supercooled liquids, as in the dielectric relaxation data. This point is elegantly confirmed by some recent data on glycerol polarized by applied fields in an interesting geometry, a piezoelectric shell [34]. Fits to the frequency-dependent bulk modulus gave $\beta = 0.43\ (2)$, in other words, $\beta = \beta_K = 3/7$, just as for KCN in the absence of coupling to the double layer. Those who are skeptical of the microscopic theory may wish to note that, although most of the discussed data are older than the theory, these results are more recent. The authors themselves note the discrepancy between the $\mathbf{F}_a = \mathbf{0}$ (specific heat, etc.) data ($\beta = \beta_{SR}$) and their large $\mathbf{F}_a$ data ($\beta = \beta_K$), and comment that it is puzzling that the two measurements yield different β's but essentially the same $\omega_0(T)$. The microscopic model has not only resolved this discrepancy, but also it has actually predicted the measured values $\beta_{SR}(\mathbf{F}_a = \mathbf{0})$ and β_K (large $\mathbf{F}_a$), in excellent agreement with experiment [34].

A minor but interesting aspect of dominant double-layer coupling at low frequencies is that it can easily produce secondary dielectric relaxation resonances. An example is provided by dielectric relaxation in several polymers, including polypropylene glycol (PPG) [35,36]. At higher temperatures multiple α resonances have been observed which have been ascribed to different kinds of segmental relaxation [37]. An alternative and, to our taste, more plausible interpretation ascribes the weaker α resonances to weakly depolymerized double layers. (Note that the multiple resonances appear to converge toward a common resonance at $T \to T_g$.) In the surfactant layer the left-handed and right-handed PPG isomers may develop additional short-range order which gives rise to additional resonances beyond that of the dipolar tilt mode found in KCN and glycerol. These extra resonances can cause confusion in empirical scaling analyses [36]. Such resonances could even appear below the bulk polymeric glass transition temperature [35].

Another minor point is the dielectric relaxation of orientationally disordered lattices such as the crystalline phase of cyclo-octanol [38]. Over a rather narrow temperature range (160–210 K), $\beta_\sigma(T)$ decreases from ~ 0.8 to ~ 0.65, which behavior is similar to that of polar organics. No evidence was obtained which would suggest approach to an orientational glass transition plateau, and the value of $\beta \sim 0.7$ at low frequencies still could be indicative of a large value of $T - T_g$.

VI. CONCLUSIONS

Although the phenomenon of stretched exponential relaxation was first identified by Kohlrausch nearly 150 years ago, there is still considerable confusion regarding its microscopic significance. In the case of fused salts dielectric relaxation near the glass transition is clearly anomalous because of the discrepancies in relaxation times between τ_σ and τ_α as measured in the absence of a large applied field. Thus one would expect that the extra channel responsible for the reduction in τ_σ by several or-

ders of magnitude compared to τ_α can also explain $d\beta/dT<0$ in dielectric relaxation. We have seen that this is indeed the case, and that dielectric double layers, well known to electrochemists for almost 100 years, are just what is needed to explain both the τ_σ and $d\beta/dT$ anomalies in KCN.

When stretched exponentials fits the relaxation of a given observable, the fit is generally excellent and economical. Such a fit requires background subtraction and proper normalization, and often measurements over a wide temperature range together with the time-temperature superposition principle [31]. This in turn will be successful if $\beta(T)$ has a low-frequency, low $T-T_g$ plateau. The width of this plateau varies from material to material and its is generally wider for better glass formers. Such a plateau exists for KCN providing we measure β by some method [25], other than dielectric relaxation, which does not couple strongly to the double layer. In nonpolar materials, such as Se, the plateau is easily recognized [1,2], The present discussion suggests that $\beta(T)$ does indeed generally have the form shown in Fig. 1(b) in the absence of extrinsic double-layer relaxation.

The situation for polar organics is generally strikingly similar to that for fused salts. In particular, dielectric relaxation in polar organics [29] is anomalous at low frequencies and crosses over at higher frequencies (AB in Fig. 3) to the expected bulk behavior of supercooled polar liquids near the glass transition. In the absence of applied fields $\beta\sim\beta_{\rm SR}$, which is similar to the fused salt value as measured by spin-polarized neutron spectroscopy. Again these differences all appear to have no systematic microscopic origin when β is viewed only as a fitting parameter, but they form a systematic pattern when viewed in the context of the present microscopic theory. This pattern itself testifies to the high quality, care, and precision of experimental design and execution which is characteristic of many efforts in this often underated field.

ACKNOWLEDGMENT

I am grateful to T. Kovacs for the least-squares fit shown in Fig. 3.

[1] Ch. Simon, G. Faivre, R. Zorn, F. Batallan, and J. F. Legrand, J. Phys. I (France) **2**, 307 (1992).

[2] R. Böhmer and C. A. Angell, Phys. Rev. B **45**, 10 091 (1992). A subtle and very sophisticated aspect of structural relaxation in a-Se, with mean coordination number $\langle r\rangle=2.0$, and Ge-Se-As alloys with $\langle r\rangle=2.1$, is that a short-time β_S and a long-time β_L can be distinguished by very carefully designed experiments, R. Böhmer and C. A. Angell, Phys. Rev. B **48**, 5857 (1993); Mater. Sci. Forum **119-121**, 485 (1993). Only β_L is measured in most experiments, and it is β_L that is believed to be chain-related. As for β_S, it is approximately 0.60 (10), and it has been ascribed to relaxation of Se_8 rings by Böhmer and Angell. The relaxation of such rings is expected to be described by $\beta_{\rm SR}$, and this is in excellent agreement with the measured value of β_S, as pointed out to us by R. Böhmer (private communication). However, it may seem surprising that the ultra-short-time relaxation measured in neutron spin-echo studies (see Ref. [1]) corresponds to β_L and not β_S. Note, however, that the latter experiments were done at higher temperatures in the supercooled liquid where Se_8 rings have probably disappeared.

[3] A. T. Ogielski, Phys. Rev. B **32**, 7384 (1985).

[4] J. N. Roux, J. L. Barrat, and J.-P. Hansen, J. Phys. Condens. Matter **1**, 7171 (1989).

[5] C. T. Moynihan, A. J. Easteal, M. A. Debolt, and J. C. Tucker, J. Am. Ceram. Soc. **59**, 16 (1976).

[6] F. Mezei, J. Non-Cryst. Solids **131-133**, 317 (1991).

[7] F. S. Howell, R. A. Bose, P. B. Macedo, and C. T. Moynihan, J. Phys. Chem. **78**, 639 (1974); J. H. Ambrus, C. T. Moynihan, and P. B. Macedo, *ibid.* **76**, 3287 (1972).

[8] J. C. Phillips, J. Non-Cryst. Solids **172-174**, 98 (1994); **182**, 155 (1995); and (unpublished).

[9] C. A. Angell and L. M. Torell, J. Chem. Phys. **78**, 937 (1983).

[10] M. Fuchs, W. Götze, and A. Lutz, Chem. Phys. **149**, 185 (1990).

[11] L. M. Torell, L. Börjesson, and M. Elmroth, J. Phys. Condens. Matter **2**, 5A207 (1990).

[12] C. P. Lindsey and G. D. Patterson, J. Chem. Phys. **73**, 3348 (1980).

[13] R. Rammal, J. Phys. (Paris) **46**, 1837 (1985).

[14] I. A. Campbell, Europhys. Lett. **21**, 959 (1993). This model is based on the concept of ring frustration (or damage) spreading under heat bath dynamics, which was first discussed by J. C. Phillips, Phys. Rev. B **31**, 3179 (1985).

[15] I. A. Campbell and L. Bernardi, Phys. Rev. B **50**, 12 643 (1994).

[16] R. J. Roe, J. Non-Cryst. Solids **172-174**, 77 (1994).

[17] H. Teichler, Phys. Status Solidi B **172**, 325 (1992).

[18] G. Ghosh, J. Mater. Res. **9**, 598 (1994).

[19] G. Gouy, J. Phys. **9**, 457 (1910); D. L. Chapman, Philos. Mag. **25**, 475 (1913); P. Debye and E. Hückel, Z. Phys. **24**, 742 (1923).

[20] A. J. Bard *et al.*, J. Phys. Chem. **97**, 7147 (1993).

[21] S. R. Peck *et al.*, J. Am. Chem. Soc. **114**, 6771 (1992); J. T. McDevitt, D. R. Riley, and S. G. Haupt, Anal. Chem. **65**, 535A (1993); J. C. Phillips, Phys. Rev. B **51**, 15 402 (1995).

[22] L. Gómez and H. T. Diep, Phys. Rev. Lett. **74**, 1807 (1995).

[23] L. T. Cheng, Y. X. Yan, and K. A. Nelson, J. Chem. Phys. **91**, 6052 (1989).

[24] R. Weiler, R. Bose, and P. B. Macedo, J. Chem. Phys. **53**, 1258 (1970).

[25] E. A. Pavlatou, A. K. Rizos, G. N. Papatheodorou, and G. Fytas, J. Chem. Phys. **74**, 224 (1991).

[26] F. Mezei, W. Knaak, and B. Farago, Phys. Rev. Lett. **58**, 571 (1988).

[27] M. Balkanski, M. K. Teng, and M. Nusimovici, Phys. Rev. **176**, 1098 (1968).

[28] Raman-scattering provides some spectroscopic evidence in support of a high concentration of such mixed complexes in KCN. The Raman- and infrared-active E' mode of the NO_3^- ion labeled ν_3 has the peak values 1380 cm^{-1} (KNO_3 melt), 1415 cm^{-1} [$Ca(NO_3)_2$ melt], and 1355 and 1480 cm^{-1} (KCN melt) according to S. C. Wait, Jr., A. T. Ward, and G. J. Janz, J. Chem. Phys. **45**, 133 (1966), and W. H. Leong, D. W. James, and M. T. Carrick, J. Raman Spectrosc. **14**, 11 (1983). Thus in the KCN melt the K and Ca bands are both present, but they have been pushed apart, which can occur only when pure complex form small clusters which interest strongly via mixed complexes at cluster interfaces.

[29] G. F. Signorini, J. L. Barrat, and M. L. Klein, J. Chem. Phys. **92**, 1294 (1990).

[30] G. E. McDuffie and T. A. Litovitz, J. Chem. Phys. **37**, 1699 (1962); P. W. Drake, J. F. Dill, C. J. Montrose, and R. Meister, *ibid.* **67**, 1969 (1977); K. L. Ngai, C. H. Wang, G. Fytas, D. L. Plazek, and D. J. Plazek, *ibid.* **86**, 4768 (1987); C. A. Angell and D. L. Smith, *ibid.* **86**, 3845 (1982).

[31] N. O. Birge, Phys. Rev. B **34**, 1631 (1986).

[32] Y. H. Jeong, S. R. Nagel, and S. Bhattacharya, Phys. Rev. A **34**, 602 (1986).

[33] P. K. Dixon, L. Wu, S. R. Nagel, B. D. William, and J. P. Carini, Phys. Rev. Lett. **65**, 1108 (1990); P. K. Dixon, Phys. Rev. B **42**, 8179 (1990).

[34] T. Christensen and N. B. Olsen, Phys. Rev. B **49**, 15 396 (1994). This paper notes that the normalized bulk modulus, but not the normalized compressibility, is well fit by the Kohlrausch function for their geometry. In general, microscopic theory cannot explain the interplay between macroscopic and microscopic constraints, specially for polar liquids at low frequencies where double layers can be important. However, microscopic theory does impose certain conditions for intrinsic relaxation, and these conditions (which essentially involve decoupling of the internal bulk relaxation from external relaxation) can be met by one observable and not another. Once this observable has been identified, microscopic theory then becomes a powerful guide for analyzing temperature and frequency dependences, as well as identifying the nature of the forces involved in the dominant microscopic relaxation modes. In the present case we believe that the piezoelectric shell polarizes glycerol ($CH_2OH{\cdot}CHOH{\cdot}CH_2OH$) by coupling of stray electric fields to the CHOH group. The polarization occurs at high temperatures when the vcell is filled, and it persists as the liquid is supercooled. Because **D** is continuous and glycerol is almost incompressible, the coupling of the applied field to low-frequency relaxation modes may be much stronger in the region of the overflow tube than elsewhere, making the glycerol in that region much more ionic than in specific heat or ultrasonic experiments [29], and shifting β from β_{SR} in the latter to β_K in the former.

[35] G. P. Johari, Polymer **27**, 865 (1986).

[36] N. Menon and S. R. Nagel, Phys. Rev. Lett. **71**, 4095 (1993).

[37] K. L. Nagi, A. Schnönhals, and E. Schlosser, Macromolecules **25**, 4915 (1992).

[38] D. L. Leslie-Pelecky and N. O. Birge, Phys. Rev. Lett. **72**, 1232 (1994); Phys. Rev. B. **50**, 13 250 (1994).